

Controlled generation and transport of reactive species in an atmospheric pressure surface barrier discharge

Aaron Dickenson,¹ Nikolay Britun,² Anton Nikiforov,³ Christophe Leys,³ Mohammad Hasan,¹ and James Walsh¹

¹Department of Electrical Engineering & Electronics, University of Liverpool, Liverpool, UK.

²Chimie des Interactions Plasma-Surface, University of Mons, Place du Parc 23, Mons, Belgium.

³Department of Applied Physics, Ghent University, Sint-Pietersnieuwstraat 41, Technicum B4, Ghent, Belgium

Abstract: In an atmospheric pressure air surface barrier discharge (SBD) the generation and transport of reactive chemical species are strongly coupled. This contribution focuses on the spatial and temporal behaviour of Reactive Oxygen and Nitrogen Species (RONS) produced by an air SBD. Laser induced fluorescence, particle imaging velocimetry and numerical modelling were used to probe RONS transport mechanisms and to identify opportunities to control the composition of RONS transported downstream of the discharge.

Keywords: Surface barrier discharge, reactive oxygen and nitrogen species, atmospheric pressure plasma, laser induced fluorescence.

1. Introduction

Reactions initiated by non-thermal atmospheric pressure plasmas in air lead to the generation of a mixture of RONS including NO, O₃, OH and H₂O₂. The ability to generate a wide variety of RONS, at room temperature using only ambient air and low cost equipment has led to an increasing interest into the possible applications of cold plasma devices in areas such as microbial decontamination, enhanced seed germination and wound therapy [1]–[3].

This study focuses on the generation and transport of RNS from a SBD given their importance in many plasma mediated healthcare applications. Laser induced fluorescence (LIF), particle image velocimetry (PIV) and computational modelling were used synergistically to explore species transport from a SBD over a wide range of operating conditions in an open air environment. Given the relatively short-lifetime of NO in the downstream effluent of a SBD, LIF was used to characterise the spatiotemporal behaviour of NO in the downstream region of the discharge with high resolution. The transport of chemical species in a SBD is primarily driven by convection, arising from the presence of electrohydrodynamic forces in the discharge [4], [5]. To quantify the influence of convection on the spatial distribution of NO, PIV was used to measure the induced flow field under different plasma operating conditions. In addition, a 2D numerical model, validated using the NO measurements and PIV flow measurements, was used to determine the spatial distribution of other key RNS beyond the discharge region and uncover the chemical pathways leading to their generation and consumption.

2. Experimental setup and diagnostic techniques.

A schematic representation of the SBD used in this investigation is shown in figure 1, the electrode unit consisted of a quartz sheet of 2 mm thickness, serving as a dielectric material. Electrodes were attached either side of the quartz, made from 35 μ m thick copper tape. The powered electrode was configured as two parallel strips separated by a 15 mm gap, referred to as the discharge gap. The outer edges of the powered electrode were insulated using Kapton tape to prevent plasma formation on edges beyond the discharge gap.

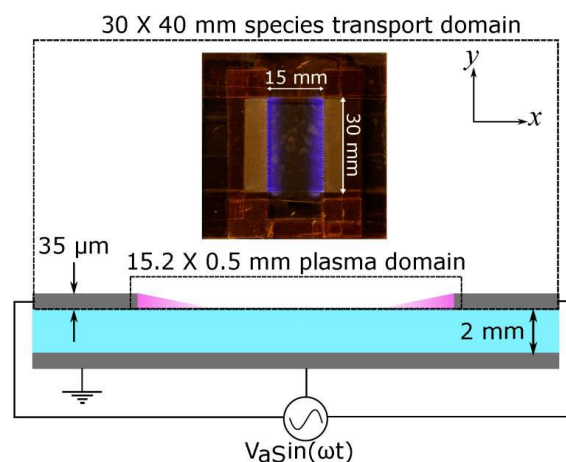


Fig. 1. Schematic showing cross-section of the surface barrier discharge used in both experimental and computational investigations (not to scale), insert shows discharge operating at an applied voltage of 15 kV.

The LIF measurement system is shown in figure 2(a). A dye laser was pumped by a 5 ns pulsed Nd:YAG laser with a wavelength of 355 nm at a repetition rate of 10 Hz. The dye laser was tuned to generate an output at a wavelength of 226.263 nm to excite ground state NO molecules. The laser pulse energy was monitored in real-time and was kept within the range of 0.07 - 0.1 mJ. A cylindrical lens was used to convert the dye laser output into a 13 mm sheet propagating perpendicularly above the discharge. To capture the fluorescence of excited NO molecules, an iCCD camera was fitted with a UV Nikkor 50 mm imaging lens via an optical bandpass with a centre wavelength of 250 nm to capture the fluorescence signal at \sim 248 nm. The camera arrangement was positioned to face the centre of the discharge gap between the two driven electrodes. To obtain calibration data, the same experimental setup was used with the exception of the SBD being replaced with a sealed chamber filled with ultra-pure helium at pressures of 300, 500, 700, and 900 mbar plus an admixture of 100 ppm of NO.

In order to quantify the flow field created by the SBD high speed PIV measurements were undertaken using the

experimental setup shown in figure 2 (b). The SBD was inserted into a large chamber seeded using oil droplets with a nominal size of 1 μm . The Stokes number of the seeding particles used throughout the study was < 0.1 , thus ensuring that the particles followed the fluid flow closely with tracing errors being $< 1\%$ [6]. A double pulsed Nd:YLF laser operating at 400 Hz with a pulse duration of 100 ns and wavelength of 527 nm was used to generate a light sheet that was projected into the seeding chamber and across the SBD electrode. A high-speed camera was positioned outside the seeding chamber perpendicularly to the laser sheet and synchronised with the laser such that each frame captured a single laser pulse. A spatial calibration was performed and the time delay between consecutive laser pulses (ΔT) was set to 20 μs , a value chosen to capture the movement of oil droplets over a square grid with spatial resolution of 56 μm , enabling the velocity vectors to be computed using a recursive cross-correlation technique.

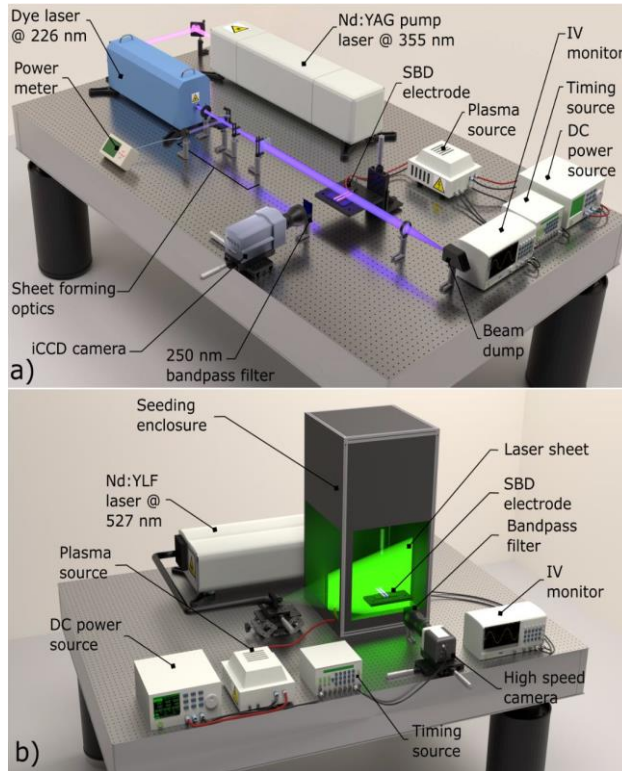


Fig. 2. Schematic showing arrangement of (a) Laser induced fluorescence experiment and (b) Particle imaging velocimetry experiment.

3. Results

To study the spatiotemporal evolution of NO generation and transport from the SBD the discharge was pulse modulated with a period of 50 ms and duty cycle of 50%. During the discharge on-time, the spatial distribution of NO and the EHD induced velocity field were measured in a region that extended 10 mm from the dielectric surface and 1 mm either side of the discharge gap. From the PIV measurements a vertical jet was observed to form resulting

from the interaction of the opposing horizontal flows at the centre of the discharge that expanded as it propagated away at a velocity of 1 m/s in a direction perpendicular to the dielectric surface, as shown in figure 3(a).

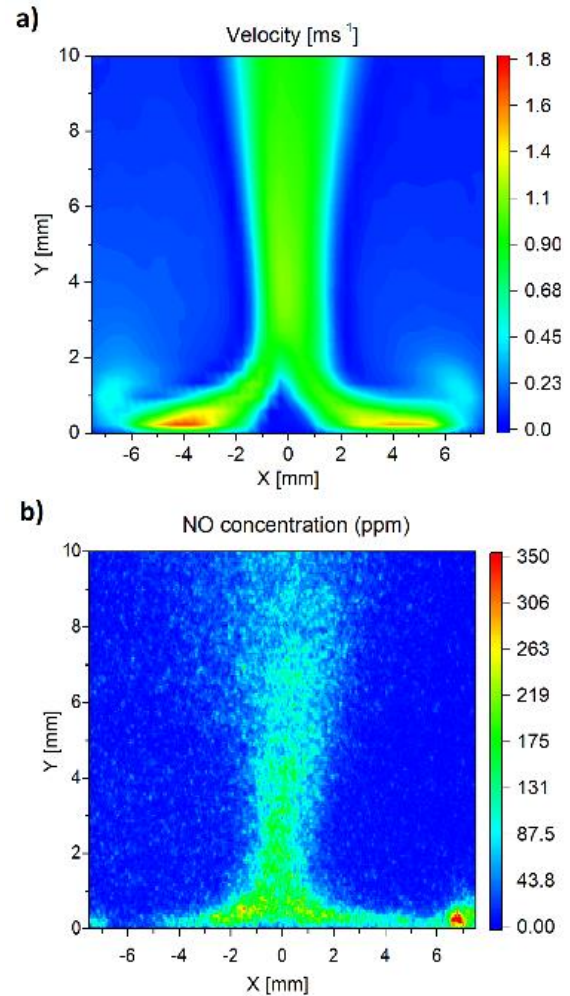


Fig. 3. (a) Steady state velocity profile at an applied voltage of 13 kV, and (b) steady state NO concentration profile at an applied voltage of 13 kV.

The steady state NO concentration measured using LIF is shown in figure 3(b). Following application of the high voltage signal ground state NO within the vicinity of the electrodes rose to approximately 300 ppm. Notably, a close correlation can be observed between the profile of ground state NO density and the spatial profile of the induced gas flow. As NO molecules are transported vertically away from the dielectric surface the concentration dropped from approximately 300 ppm at the surface to approximately 50 ppm at a distance of 6 mm above the dielectric surface. Following termination of the plasma, NO concentration across the dielectric surface was observed to drop rapidly, while downstream of the dielectric surface several tens of ppm remained. These measurements indicate that the loss rate of NO in the vicinity of the dielectric surface is greater than that away from the surface. The correlation between

LIF and PIV measurements clearly demonstrates that the induced EHD force and the generation of NO occur at the same position (*i.e.* next to the electrode edges where the visible discharge exists) and some proportion of the generated NO is transported by convection to the centre of the discharge gap and downstream along the resultant perpendicular jet.

From the results of numerical modelling it was established that the rapid loss of NO at the dielectric surface occurring when the discharge was extinguished can be explained by two factors: firstly, O₃ has its highest concentration in the vicinity of the dielectric surface, meaning that the loss reaction between O₃ and NO plays a comparatively larger role in this region compared to any downstream location, resulting in a higher loss rate of NO in the vicinity of the surface. The second factor is the induced flow, which removes NO from the discharge region where it is primarily produced to the downstream region.

4. Conclusion

The reaction pathways and transport mechanisms of key reactive nitrogen species produced by a surface barrier discharge operating in open air were examined using computational modelling and experimental measurements. Particle imaging velocimetry was used to uncover the induced flow structure created by electrohydrodynamic forces generated by the SBD while laser induced fluorescence was used to obtain measurements of ground state NO concentration. Both techniques facilitated time and space resolved measurements. Steady state measurements of the discharge were used to benchmark the developed numerical model, which was then used to identify the main reaction pathways of other key reactive species.

It was shown that the induced velocity and source of NO both originated at the edge of the driven electrodes which corresponded to the visible plasma region; beyond this region the NO concentration was seen to extend into the centre of the discharge gap and vertically away from the dielectric surface, closely mirroring the measured velocity profile. Along the axis of the induced vertical jet, steady state measurements showed that the NO concentration peaked at the dielectric surface and then dropped downstream.

Overall, this study highlights that significant densities of reactive nitrogen species can be delivered significant distances downstream of a surface barrier discharge. Notably NO, which is of considerable biological importance and a key application enabler, was observed to be transported several centimetres downstream of the discharge region by the plasma induced flow. Through computational modelling the key reaction pathways responsible for the generation and loss of major reactive nitrogen species have been identified and this insight can be used to aid in the development and understanding of plasma-based healthcare devices employing the surface barrier discharge configuration.

5. Acknowledgements

JLW & MIH would like to acknowledge the support of the Engineering and Physical Sciences Research Council (Projects EP/J005894/1 and EP/N021347/1) and Innovate (Project 50769-377232). NB acknowledges the support of the REFORGAS GreenWin project (grant No. 7267).

6. References

- [1] M. Modic, N. P. McLeod, J. M. Sutton, and J. L. Walsh, "Cold atmospheric pressure plasma elimination of clinically important single- and mixed-species biofilms," *Int. J. Antimicrob. Agents*, vol. **49**, no. 3, pp. 375–378, (2017).
- [2] X. Q. Wang, R. W. Zhou, G. De Groot, K. Bazaka, A. B. Murphy, and K. K. Ostrikov, "Spectral characteristics of cotton seeds treated by a dielectric barrier discharge plasma," *Sci. Rep.*, vol. **7**, no. 1, pp. 1–9 (2017).
- [3] S. Kubinova, K. Zavisikova, L. Uherkova, V. Zablotskii, O. Churpita, O. Lunov, and A. Dejneka, "Non-thermal air plasma promotes the healing of acute skin wounds in rats," *Sci. Rep.*, vol. **7**, no. March, pp. 1–11, 2017.
- [4] A. Dickenson, Y. Morabit, M. I. Hasan, and J. L. Walsh, "Directional mass transport in an atmospheric pressure surface barrier discharge," *Sci. Rep.*, vol. **7**, no. 1, pp. 1–9, 2017.
- [5] M. I. Hasan, Y. Morabit, A. Dickenson, and J. L. Walsh, "Impact of electrode geometry on an atmospheric pressure surface barrier discharge," *Appl. Phys. Lett.*, vol. **110**, no. 26, pp. 1–5, 2017.
- [6] R. D. Whalley and J. L. Walsh, "Turbulent jet flow generated downstream of a low temperature dielectric barrier atmospheric pressure plasma device," *Sci. Rep.*, vol. **6**, July, pp. 1–7, 2016.